Global phytoplankton standing and propagating ENSO variability signals from satellite derived chlorophyll-*a*

André B. Couto[1] and Angela M. Maharaj[2]

Abstract —Understanding how propagating signals influence phytoplankton distribution at the euphotic layer is a subject of enormous scientific interest. The proposed mechanisms range from meridional advection, uplift/downlift of the community, and upwelling/downwelling of nutrients. These will increase phytoplankton in a specific area by either gathering them or allowing better conditions for reproduction (i.e., increased access to light or nutrients). It is known that ENSO and its associated propagation play a significant role on ocean circulation and climate variability. In the present study we provide empirical evidence of an immediate and lagged influence of ENSO on SeaWiFS and MODIS Aqua derived global Chlorophyll *a* concentrations (Chl). We demonstrate that the influence of ENSO on phytoplankton dynamics occurs in well defined oceanic regions, which are neither restricted to the Tropical Pacific nor to a specific timeframe. Chl distributions suggest that zonal phytoplankton communities react in different phases to the shoaling/deepening of the thermocline. An analysis of propagating signals suggests that ENSO driven propagation explains a substantial amount of interannual phytoplankton variability throughout the Tropical Pacific. Thus, to better understand the importance of ENSO on phytoplankton distribution, further work has to be done on ENSO driven propagation and its associated dynamics.

Keywords — ENSO, Propagation, Satellite derived chlorophyll-*a*

1 Introduction

El Niño - Southern Oscillation (ENSO) is a Tropical Pacific phenomenon with worldwide climatic teleconnections. Despite the unknown relationship between ENSO and global warming, several studies have also linked an increase in the amplitude of ENSO [1], as well an increase in the predominance and intensity of the El Niño phase of ENSO to global warming [2]. ENSO is a coupled atmosphere-ocean system that occurs in the Tropical Pacific. Its oscillation, driven by the Walker circulation [3], determines the state of ocean physical characteristics, such as the mixed layer depth. The mixed layer depth is crucial for phytoplankton, since it determines the abundance of nutrients in the euphotic depth, where these photoautotroph organisms are limited to live. In this study we aim to investigate how global phytoplankton patterns are distributed, in space and time, due to ENSO dynamics. Remote sensing tools have proven to overcome the greatest limitations that classical observational methods suffer by providing global coverage and a continuing sampling rate. Sensors such as the recently terminated SeaWiFS project and the on-going MODIS *Aqua*, are passive ocean colour instruments that measure water leaving radiance which can be converted into Chlorophyll-*a* (Chl) concentrations. Due to the presence of this molecule in all phytoplankton organisms, Chl is commonly used as a phytoplankton biomass indicator throughout the water column.

2 Data and Methods

The Multivariate ENSO Index (MEI) represents ENSO atmosphere-ocean interactions by taking into account six observed variables over the Tropical Pacific. These are: sea level pressure, both components of surface wind, sea surface temperature, surface air temperature, and total cloudiness fraction of the sky [4]. The MEI is the time series of the leading mode yielded when performing an empirical orthogonal function (EOF) analysis of all six fields together. A negative/positive index period is related to a La-Niña/El-Niño event, i.e., a cold/warm ENSO phase respectively.

Remote sensing has proven to be an ideal observational tool, since it provides a continuous sampling of the global ocean. In this study we use SeaWiFS, from October 1997 to December 2007, and MODIS Aqua, from January 2008 to October 2010, monthly averaged global ocean maps of Chl observations. These maps represent, in their original grid form, 18 km^2 per pixel at the equator, reducing zonally towards the poles, then were interpolated to a four times larger grid, i.e., to a 72 km^2 at a latitude of 0º. Chl maps were converted

1. *A. B. Couto is with the Department of Environtment and Geography, Macquarie University, Sydney, 2109 NSW, Australia. E-mail: Belo.Couto@gmail.com*
2. *A. M. Maharaj is with the Department of Environtment and Geography, Macquarie University, Sydney, 2109 NSW, Australia. E-mail: angela.maharaj@mq.edu.au*

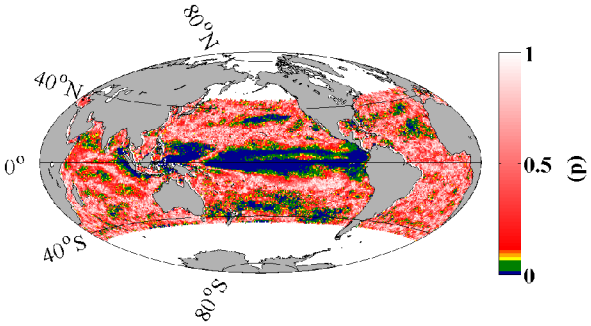

Fig. 1. Significance (p-value) of the probability that MEI has the same distribution as Chl time series for each grid point (p), green are values between 0.01 and 0.1. Calculated with reduced number of intervals [5].

to log-distribution and monthly averages were then subtracted from the time series, which was then divided by its standard deviation to normalise the intra-annual cycles of the Chl values. The data was smoothed over each three months prior to being detrended. Posterior analysis was only performed on grid points which had full time coverage, i.e., n=157. Additionally, all correlations between MEI and each grid point time series were estimated using a reduced number of degrees of freedom [5]. Cross-correlation were carried out to determine the time lag of the best fit between MEI and each Chl grid point time series.

The classical Empirical Orthogonal Function (EOF) is a common mathematical tool used in atmospheric sciences to identify the patterns that explain most of the variability within a set of observations [6]. While the technique yields a standing wave-like pattern, propagating signals are often isolated into different modes with a similar temporal series. Furthermore, if the data is truncated into a series of predefined lag times prior to performing the EOF, the result isolates modes that explain all the variance within a propagation mode that best fits the predefined lag. This method is called an extended EOF (EEOF) and is commonly used to study propagating features in atmospheric sciences [7]. Here, we use it to isolate oceanic Chl propagation that occurs with the same cycle as the MEI maximum spectrum (L = 28 months).

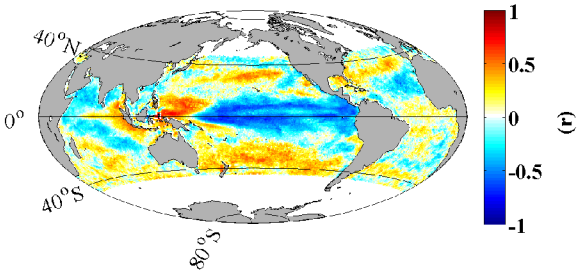

Fig. 2. Coefficient relation (r) when testing the relationship between MEI and Chl time series for each grid point.

3 Results

Fig. 1 shows the spatial distribution of statistical significance between the MEI and Chl time series. ENSO has a more significant influence on Chl concentrations over the Pacific then in other ocean basins. Nevertheless, significant relationships are also found in the Indian Ocean (mainly off the Java and Sumatra west coasts) and within the centre of the North Atlantic gyre (Fig. 1). Furthermore, significant relationships are found to exist not only in the Tropical region of the Pacific but also further poleward to 35° in both hemispheres. These extra-tropical regions also display high correlation coefficients, albeit with an inverse relationship to that observed throughout the Tropical Pacific, with the exception of the west side of the basin where a positive correlation coefficient is observed (Fig. 2). Direct and highly significant relationships are also found in the subtropical regions.

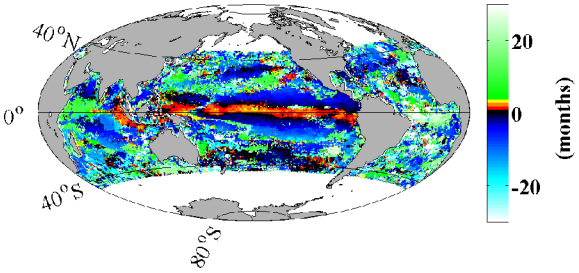

Fig. 3. Time lag (months) of best coefficient correlation (r) between MEI and Chl time series for each grid point. Positive values mean that Chl is leading.

Interestingly, while all these Chl regions track well with the MEI, they display different timing with respect to a best fit with the ENSO signal. As we can see in Fig. 3, the Chl temporal series over the Equatorial Pacific and also at the west coast of Java and Sumatra in the Indian basin (with either a direct or inverse relation to the MEI) has a positive (leading) best fit to the MEI, and in some regions at three or more months earlier. This best fit is delayed towards the poles. However, in the mid latitude Pacific where a significant relationship with the MEI is observed, the best correlation fit occurs simultaneously with the MEI. The same best fit of near zero lag occurs between the MEI and Chl patterns in the North Atlantic gyre.

The EOF analysis yielded two independent modes of variability [8] with time coefficients that are significantly related to the MEI: EOF mode 2 at $r = 0.83$ ($p << 0.01$), and the third EOF mode with a MEI lead lag of 8 months for the best fit ($r = -0.76$, $p << 0.01$) (Fig. 4). These two modes together explain 14% of the Chl inter-annual variability, mostly in the Tropical Pacific region and off the west coasts of Java and Sumatra. However, the

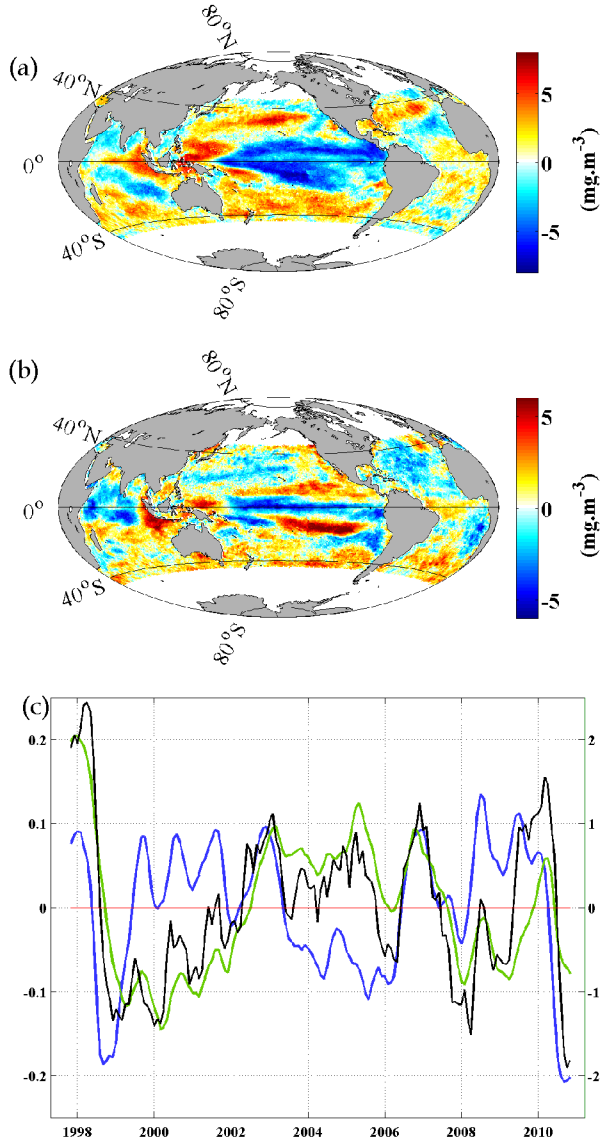

Fig. 4. EOF modes that significantly related to MEI. (a) EOF mode 2 spatial pattern explaining 9% of Chl interannual variability between October 1997 and October 2010; (b) EOF mode 3 spatial pattern explaining 5% of same as the previous; (c) EOF modes 2 (blue) and 3 (green), and MEI (black) time series.

EOF mode 3 spatial pattern is quite different from the pattern in mode 2. Whereas in mode 2 the spatial pattern resembles Fig. 2, reminiscent of the same regions where Chl distribution is strongly influenced by ENSO, the mode 3 pattern shows a strong signal along the equatorial line, and an equally strong amplitude of the opposite signal northward and southward off the equator. This suggests that ENSO dynamics drive a Chl interannual variability signal at the Tropical Pacific, the spatial pattern of which is best represented by the EOF mode 3 in Fig. 4, and occurring 8 months after changes in the regional climate mode.

The EEOF analyses yielded only one mode that significantly tracked MEI, mode 2 ($r = 0.79$, $p = 0.001$), as seen in Fig. 5a. This mode explains 6% of the Chl interannual variability pattern propagating mainly along the Tropical Pacific (Fig. 5b), although, variability patterns are observed at higher latitudes of the Pacific, as well as in the North Atlantic and Indian Ocean in the same regions where a significant relationship was previously found. This propagating EEOF mode 2 has a good correlation with the spatial patterns of both EOF modes discussed before that showed a highly significant relationship with ENSO. The EOF mode 2 spatial pattern shows the best significant relationship with EEOF mode 2 at the first time step ($r = 0.96$, $p << 0.001$) of the series, whilst EOF mode 3 is better represented by EEOF mode 2 step 11 ($r = 0.63$, $p <<0.001$; Fig. 6). This not only strongly indicates that EEOF mode 2 is due to ENSO dynamics, but also confirms that EOF mode 3 is an ENSO propagation signal.

4 DISCUSSION

The near equatorial trough between the subtropical high-pressure systems located in both hemispheres at the eastern Pacific and western Atlantic accelerate air masses towards the equator, which with coriolis deflection makes the easterly trade winds. The associated wind stress will drag the warm ocean surface layer westward uncovering a deeper lower layer of nutrient rich cooler waters on the eastern side of the Equatorial

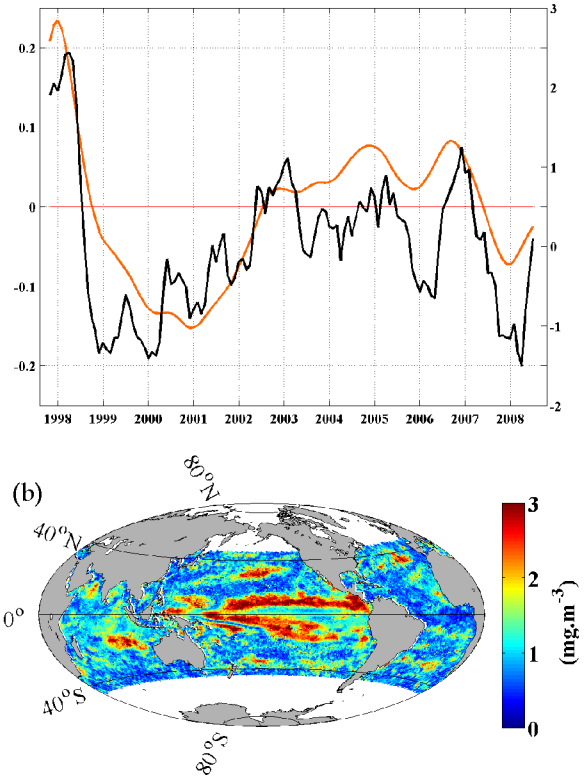

Fig. 5. EEOF mode 2 of interannual Chl: (a) EEOF time series (orange) and MEI; (b) EEOF standard deviation of mode 2.

Pacific basin, which is also dragged westward by the same force. The impact of the thermocline shoaling due to the trade wind forcing in the Eastern Tropical Pacific on phytoplankton communities [9], and also the impact of ENSO dynamics on global ocean phytoplankton distribution [10] have been previously reported. However, the influence of ENSO in phytoplankton distribution in subtropical latitudes, in either Pacific basins, or in the North Atlantic, as reported here (Fig. 1), is not clear in the current literature. Further to this, the various timing of best fits with MEI suggest that depending on the zonal location along the Tropical Pacific, phytoplankton communities have a different phase of reaction to ENSO fluctuations (Fig. 3). It is worth noting that the MEI is an index representing the entire Tropical Pacific domain [4], and not specifically reflecting propagating atmospheric or oceanic waves that occur, e.g., when ENSO is shifting phase. Nevertheless, taking the MEI as an average of propagating modes occurring throughout the Tropical Pacific, our results indicate that this index is significantly coupled and synchronous with Chl patterns that occur off the equatorial belt, and lagged with the patterns at the equator. Indeed, the EOF analysis suggests that the Chl pattern has a highly significant correlation to the MEI at an 8 month lag in addition to the dominant and synchronous pattern driven by ENSO. The ENSO related out of phase Chl variability EOF mode 3 (Fig. 4), is actually quite similar to a result reported by Behrenfeld et al., [11], as the difference between two consecutive La Niña events of similar intensity. This suggests that mode 3 might represent the signal of a persistent ENSO phase. Nevertheless, the EEOF propagation analysis includes such a pattern in its ENSO related propagation mode, in addition to the synchronously related EOF mode 2.

5 Conclusions

In summary, we demonstrate that the influence of ENSO on phytoplankton dynamics occurs in well defined oceanic regions, which are neither restricted to the Tropical Pacific nor to a specific frequency. Chl distributions suggest that zonal phytoplankton communities react in different phases to the shoaling/deepening of the thermocline. An analysis of propagating signals suggests that ENSO driven propagation explains a substantial amount of interannual phytoplankton variability throughout the Tropical Pacific. We speculate that the observed delayed reaction to ENSO variability might be due to several mechanisms, including the persistence of an ENSO phase. Thus, to better understand the importance of ENSO on phytoplankton distribution, further work has to be done on ENSO driven propagation and its associated dynamics.

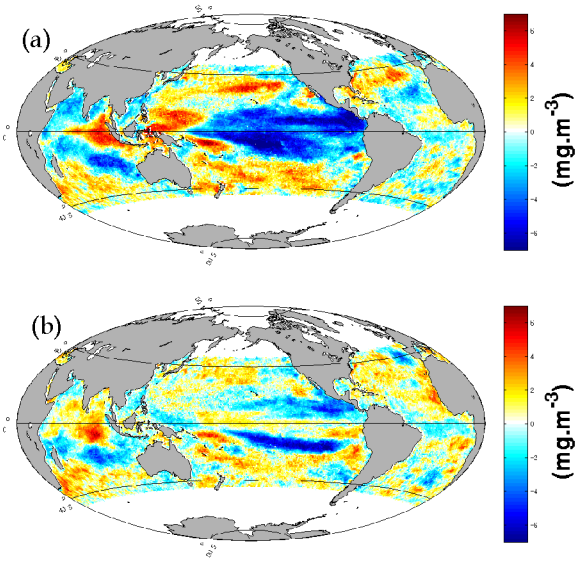

Fig. 6. Chl interanual EEOF mode 2 spatial patterns of step 1 (top) and 11 (bottom).

References

[1] Zhang Q, Guan Y, Yang H. ENSO amplitude change in observation and coupled models. Advances in Atmospheric Sciences 2008;25(3):361-6.

[2] Fedorov AV, Philander SG. Is El Niño Changing? Science 2000 June 16, 2000;288(5473):1997-2002.

[3] Wang C, Enfield DB. A Further Study of the Tropical Western Hemisphere Warm Pool. Journal of Climate 2003;16(10):1476-93.

[4] Wolter K, Timlin MS. Monitoring ENSO in COADS with a seasonally adjusted principal component index. Proc of the 17th Climate Diagnostics Workshop; 1993; Norman, OK, NOAA/NMC/CAC, NSSL, Oklahoma Clim. Survey, CIMMS and the School of Meteor., Univ. of Oklahoma; 1993. p. 52-7.

[5] Davis RE. Predictability of Sea Surface Temperature and Sea Level Pressure Anomalies over the North Pacific Ocean. Journal of Physical Oceanography 1976;6(3):249-66.

[6] Bjornsson H, Venegas SA. A manual for EOF and SVD analyses of climate data. Montréal, Québec: McGill University; 1997.

[7] Holbrook NJ, S-L CP, Venegas SA. Oscillatory and propagating modes of temperature variability at the 3–3.5- and 4–4.5-yr time scales in the upper southwest Pacific Ocean. Journal of climate 2005;18:719-36.

[8] North GR, Bell TL, Cahalan RF, Moeng FJ. Sampling Errors in the Estimation of Empirical

Orthogonal Functions. Monthly Weather Review 1982 July 01, 1982;110(7):699-706.
[9] Pennington JT, Mahoney KL, Kuwahara VS, Kolber DD, Calienes R, Chavez FP. Primary production in the eastern tropical Pacific: A review. Progress in Oceanography 2006;69(2-4):285-317.
[10] Behrenfeld MJ, O/'Malley RT, Siegel DA, McClain CR, Sarmiento JL, Feldman GC, et al. Climate-driven trends in contemporary ocean productivity. Nature 2006;444(7120):752-5.
[11] Behrenfeld MJ, Randerson JT, McClain CR, Feldman GC, Los SO, Tucker CJ, et al. Biospheric primary production during an ENSO transition. Science 2001;291(5513):2594-7.